

# Timescale of Crystal Mush Storage in the Central Southern Volcanic Zone of Chile (CSVZ)

M. Billon<sup>a</sup>, B. Charlier<sup>a</sup>, O. Namur<sup>b</sup>, J. Vander Auwera<sup>a</sup>

<sup>a</sup>University of Liège - Department of Geology, B20—4000 Liège—Belgium

<sup>b</sup>University of Leuven - Department of Earth and Environmental Sciences

Contact : melvyn.billon@uliege.be

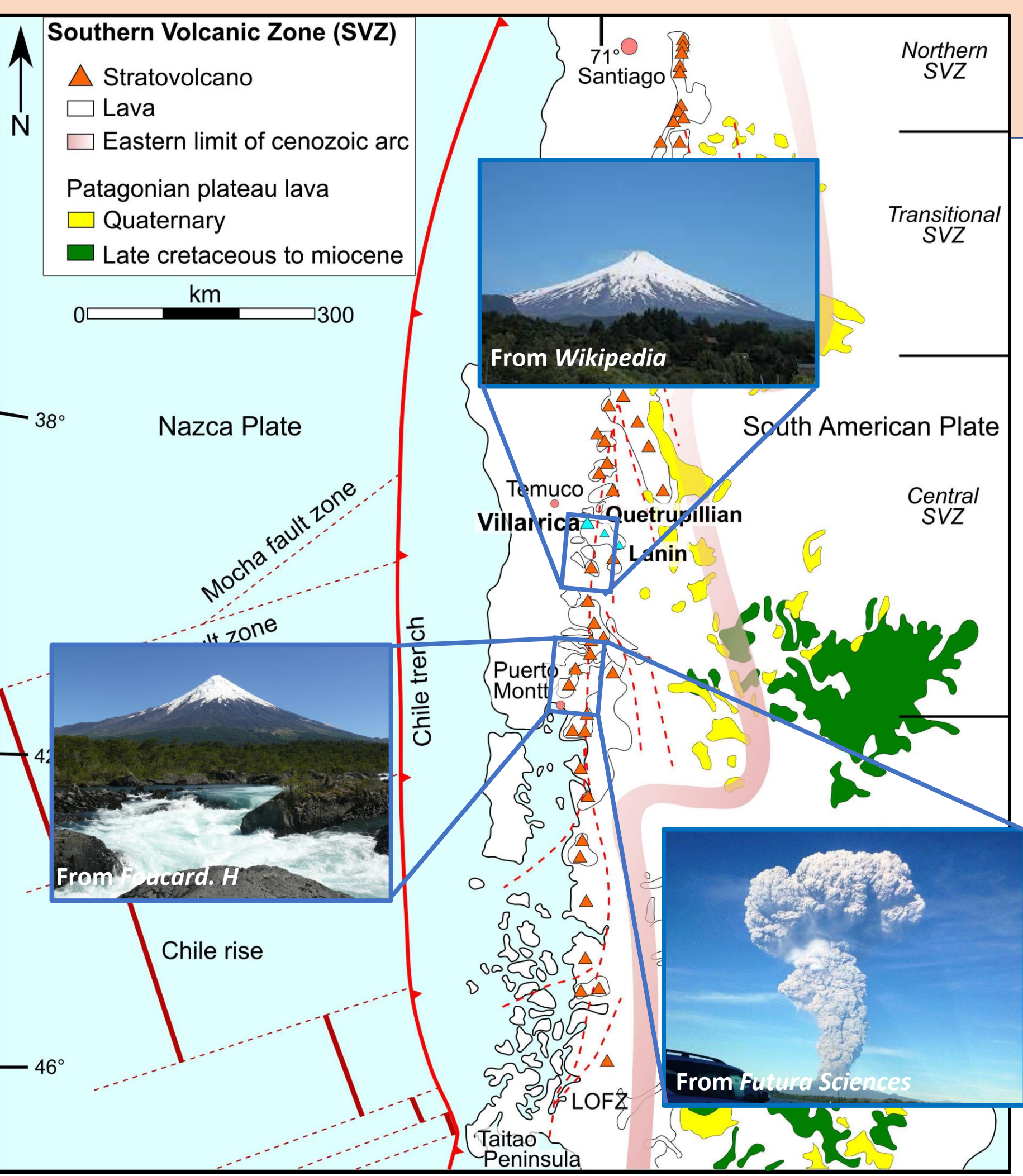


Figure 2 : Map of the Southern Volcanic Zone (modified after Stern et al., 2004) with pictures of the studied volcanoes (Osorno, Calbuco, Villarrica).

## Introduction

The magma ascent rate from the main storage region to the surface is relatively well constrained (months to years) but there is more uncertainty about the duration of differentiation within reservoirs (1000 to more than 100,000 years).

The CSD (Crystal Size Distribution) method established by Marsh (1988) is based on the evolution of the number and size of crystals as a function of the residence time (Fig. 1). The slope of a CSD depends on the growth rate and residence time of the crystals:

$$\text{slope} = \frac{-1}{G(\text{growth rate}) * t(\text{residence time})}$$

We will combine the experimental determination of the plagioclase growth rate (G) with the CSD method (slope of the CSD) applied to a selection of natural samples to estimate the duration of differentiation within these magmatic systems. Preliminary results are shown here.

This study is based on samples (Figs 2-3) from four volcanoes (Osorno, Calbuco, Villarrica, and La Picada) of the Central Southern Volcanic Zone of Chile (CSVZ), a particularly active volcanic area. Turner et al., 2016 also showed that the geochemical variability observed within the SVZ is representative of the global arc magmatism, making it a good reference area.

Figure 1 → : CSD profile allowing to go back to residence time. 't' is the residence time, and 'G' the growth rate.

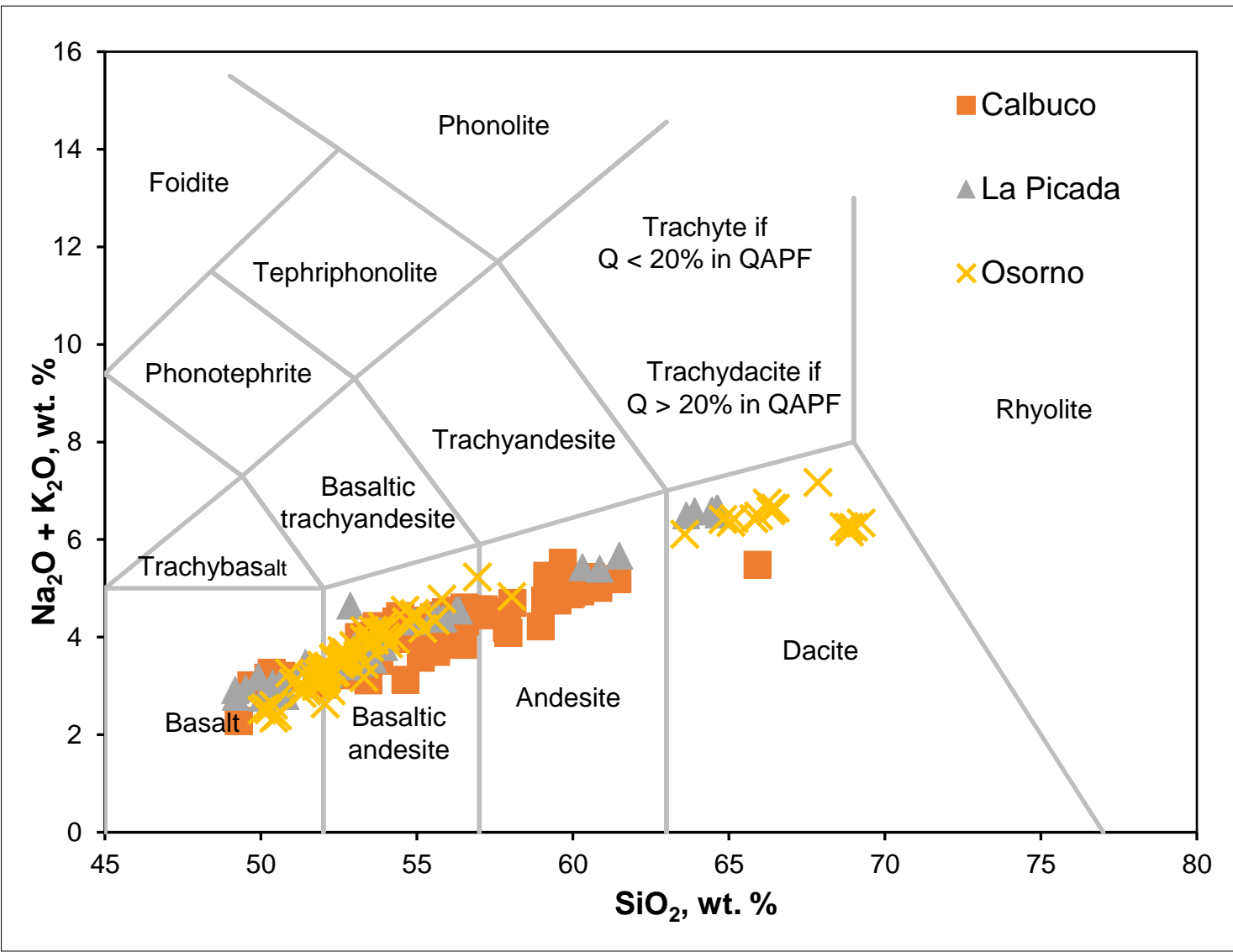
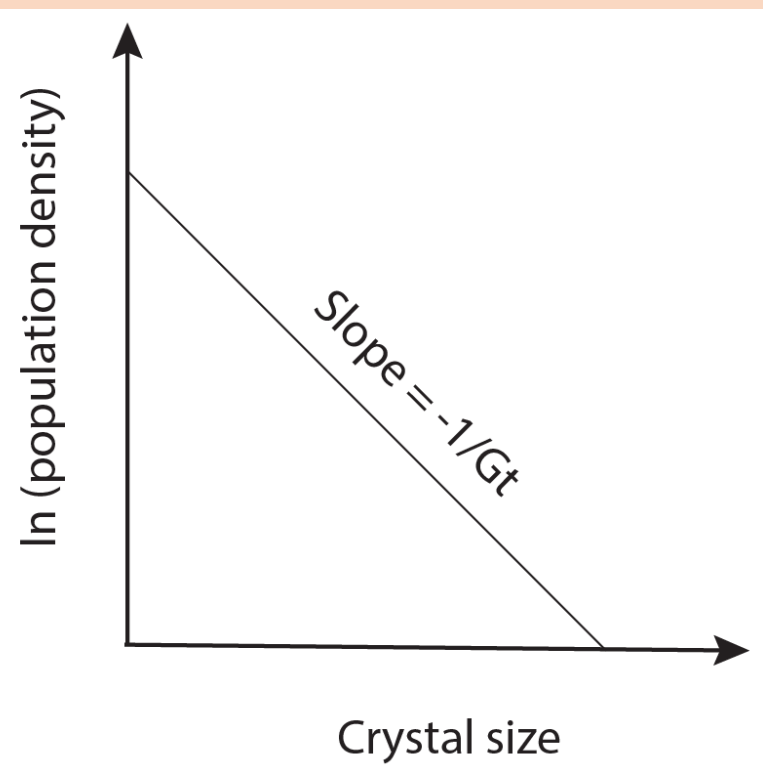


Figure 3 ↑ : TAS diagram of the samples of studied area. Most of the rocks collected are basaltic andesites.

## Experimental Method

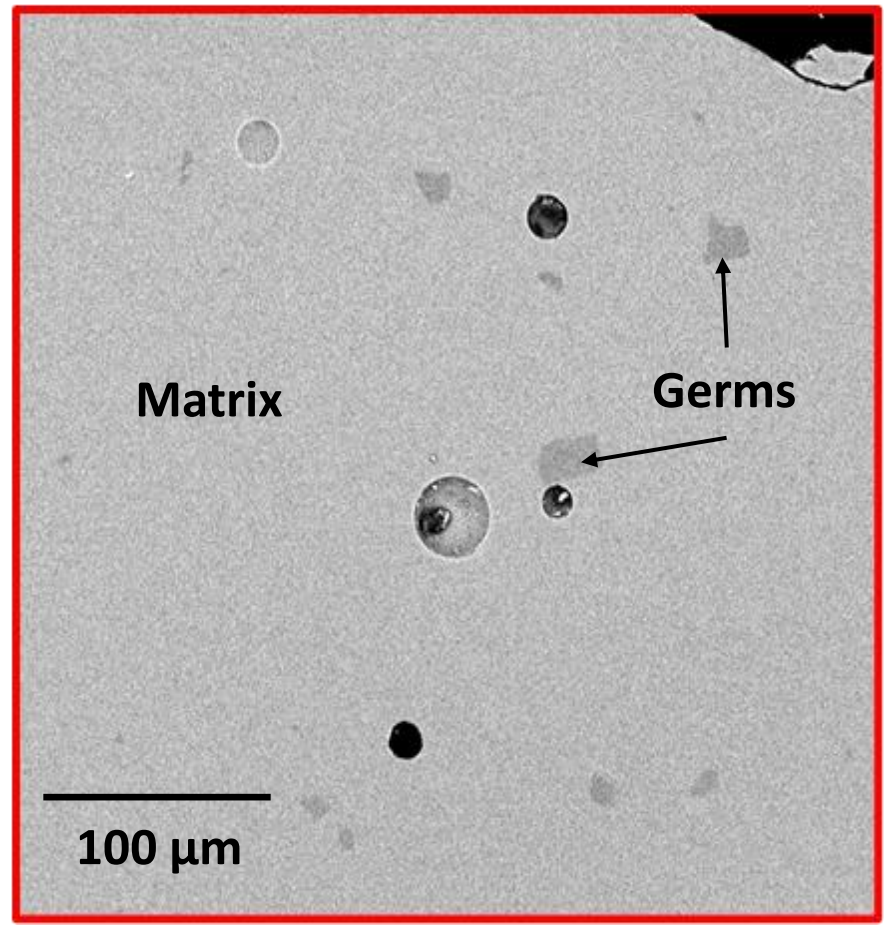
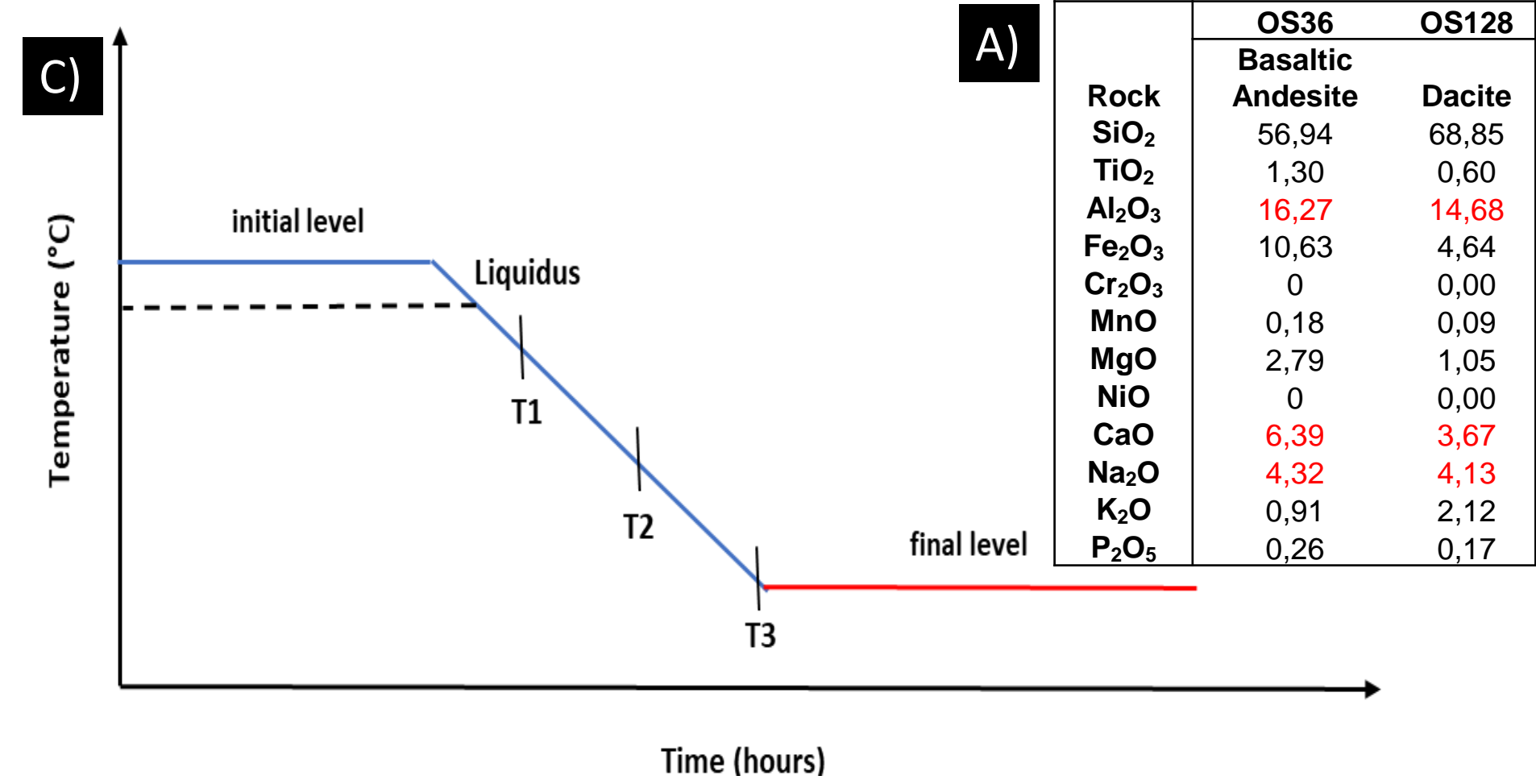
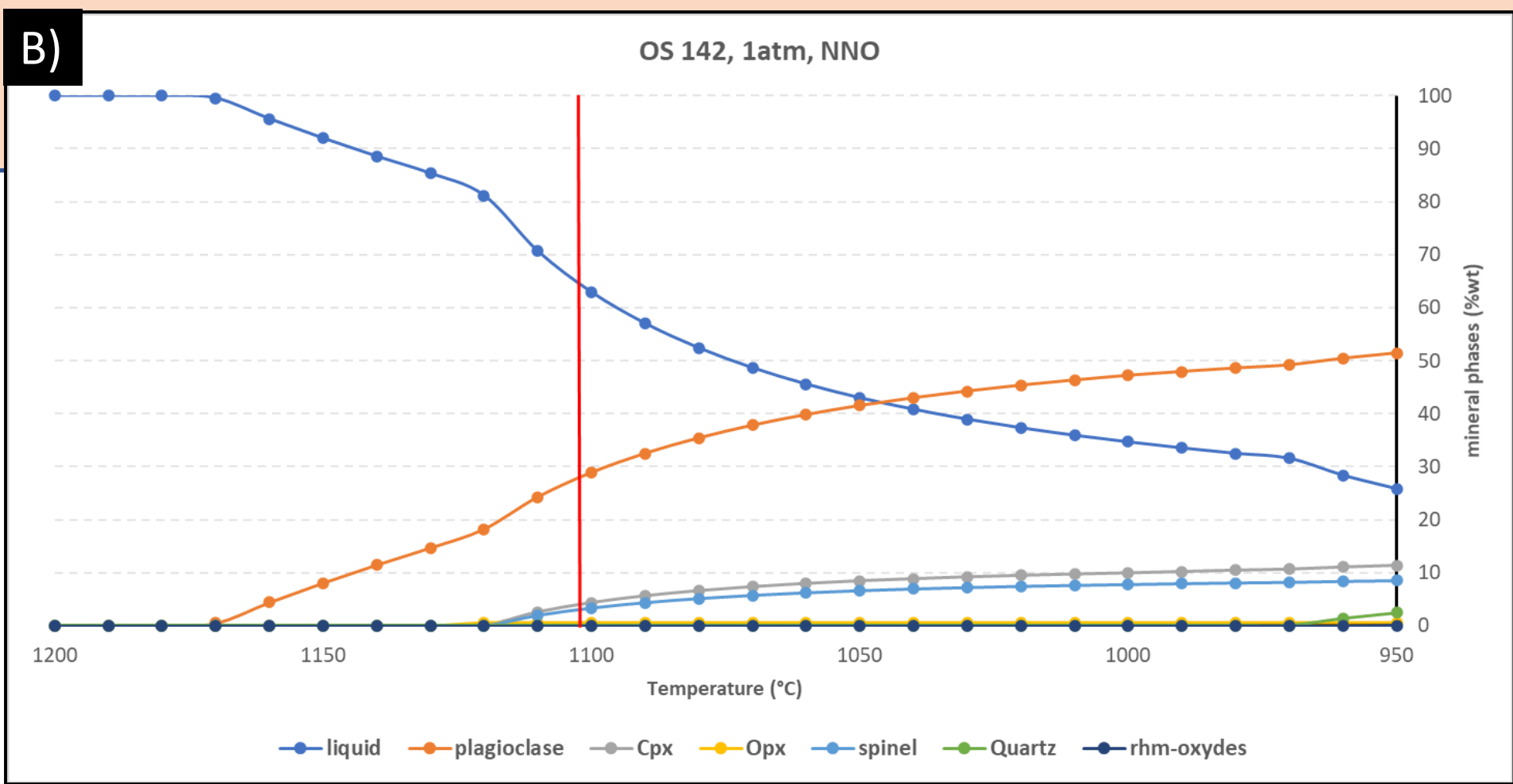


Figure 5 : BSE image of the first germs of plagioclase in the sample heated at 1190°C.

Future experiments will focus on the role of pressure, composition and initial water content on the plagioclase texture.

- A basaltic andesite and a dacite (from Osorno, Fig 4 A) were powdered, mixed with water (mud) and then heated in a muffle furnace at 1000°C to remove volatiles and most crystals (Toplis and Carroll, 1995-1996 ; Pupier, 2018).
- The plagioclase liquidus temperature was first thermodynamically determined with Rhyolite Melts (Fig 4 B-5).
- A series of experiments were run at 1 atm (ULiège, Fig 4 C) to constrain the plagioclase liquidus temperature and its growth rate at various cooling rates (1, 3, and 9°C/h) (Fig 5). Loads are quenched at 1165, 1140, 1120, and 1100°C.

Figure 4 → : A) Major element composition of the basaltic andesite and dacite. B) Thermodynamic simulation via Rhyolite-MELTS of the fractional crystallization of the basaltic andesite. C) Crystallization path followed experimentally. An initial plateau of 24 hours around the liquidus temperature, followed by a cooling slope at various rates. T1, T2, and T3 correspond to the quenching temperatures.



## Results : Evolution of Crystallinity with Cooling rate

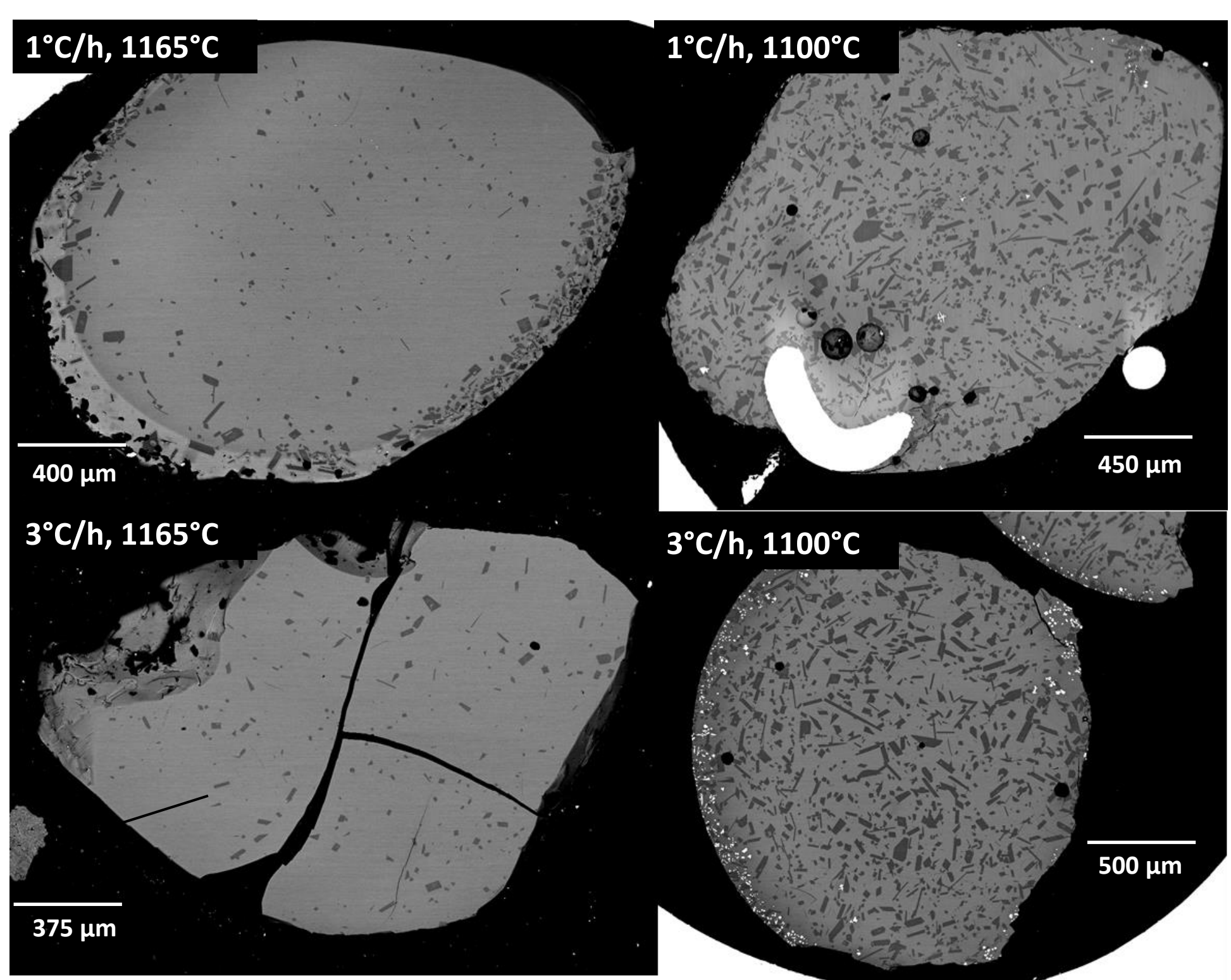


Figure 6 ↑ : BSE images of the experimental loads quenched at the start (1165°C) and end of cooling (1100°C), for cooling rates at 1°C/h, and 3°C/h.

The experimental liquidus temperature agrees with the Melts model, respectively 1190°C and 1170°C (Fig 4B and 5).

Experiments quenched at decreasing temperatures indicate spontaneous nucleation of plagioclase around 1190°C followed by crystal growth and maturation (anhedral to euhedral shape) until the final temperature T3 (Figs 6-7).

The cooling rate influences the nucleation/growth ratio, and the shape of the crystals. With increasing cooling rate, the crystal growth rate decreases in favor of the nucleation rate (high density of small crystals (Fig. 6-7). These results are in agreement with those of Gibb (1974) and Pupier (2018).

Determination of growth rate (Fig 8) :  $G_{\text{max}} = \frac{(L*W)^{1/2}}{2*t}$

- Gmax on the 10 largest crystals
- Gmean over all the crystals

Favor tomography to have the real size of the crystals (avoid corrections for transition from 2D to 3D).

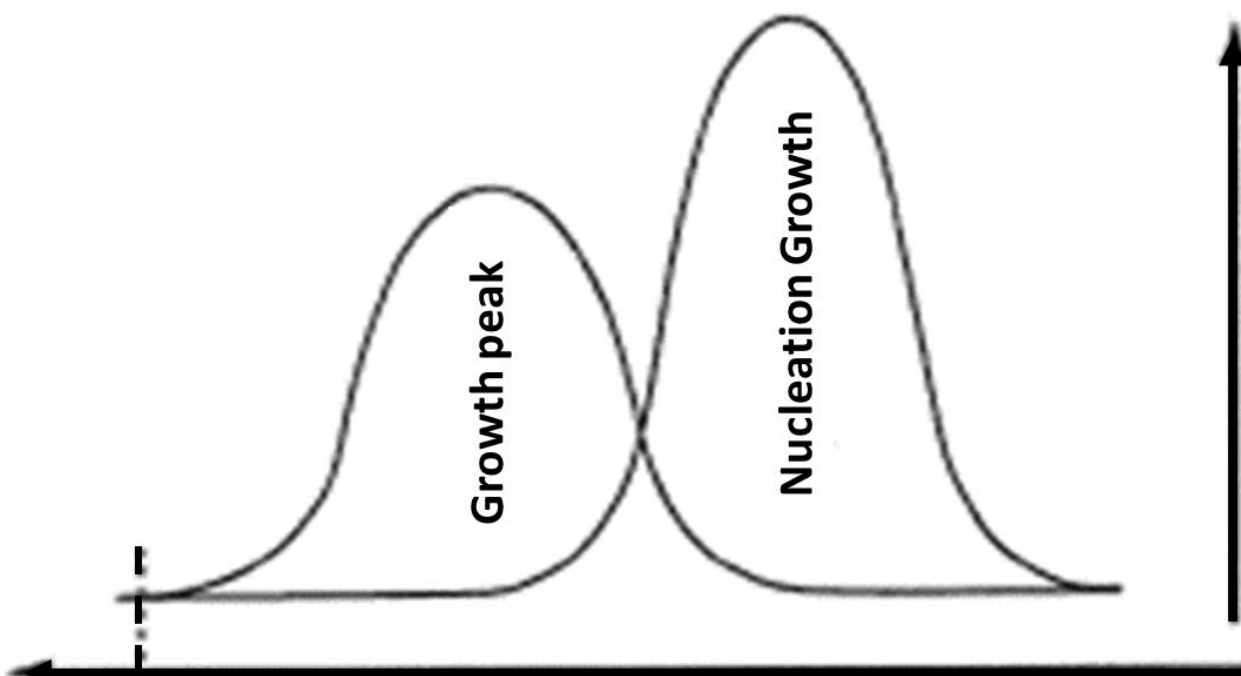


Figure 7 ← : Evolution of the nucleation/growth ratio during cooling.

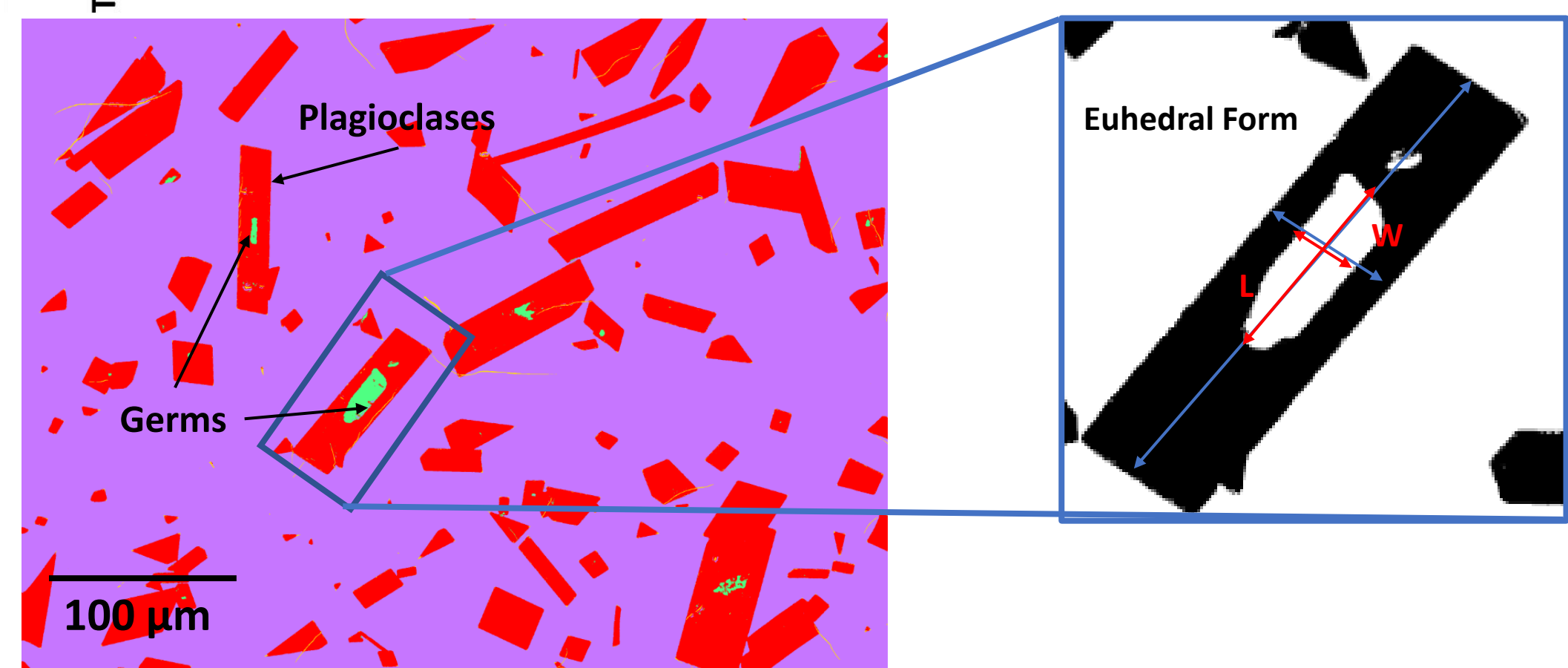


Figure 8 ↑ : Segmentation carried out via Weka Segmentation in ImageJ. On the zoom, the long (L) and short (W) axes of the mineral appear in blue, and those of the germ in red.

## References

Gibb, E.G.F (1974), 'Supercooling and the crystallization of plagioclase from a basaltic magma', Mineralogical Magazine, 39, 641-653.  
Higgins M. D. (2000), 'Measurement of crystal size distributions.' American Mineralogist, 85, 1105-1116.  
Marsh B. D. (1998), 'On the Interpretation of Crystal Size Distributions in Magmatic Systems.' Journal of Petrology, 39, 553-599.  
Pupier E. (2018), 'Approche expérimentale de la cristallisation dans les chambres magmatiques et étude d'intrusions litées (massif gabbroïque du Skaergaard, Groenland et pluton granitique de Dolbel, Niger)', PhD, Université de Lorraine - CRPG.  
Stern C. R. (2004), 'Active Andean volcanism : its geologic and tectonic setting', Revista Geologica de Chile, 31, 161-206.  
Toplis M. J., and Carroll M. R. (1996), 'Differentiation of Ferro-Basaltic Magmas under Conditions Open and Closed to Oxygen: Implications for the Skaergaard Intrusion and Other Natural Systems.' Journal of Petrology, 37(4), 837-858.